

## Modelling and Simulation of CO<sub>2</sub> Capture through Aqueous Indirect Mineralization using CaO-containing By-products

Amirhossein Ghazi\*, Lars-Andre Tokheim\*\*

\* Department of Process, Energy and Environmental Technology, University of South-Eastern Norway  
(Tel: +47 96 72 84 65; e-mail: [Amirhossein.ghazi11@gmail.com](mailto:Amirhossein.ghazi11@gmail.com))

\*\* Department of Process, Energy and Environmental Technology, University of South-Eastern Norway  
(Tel: +47 35 57 51 71; e-mail: [Lars.A.Tokheim@usn.no](mailto:Lars.A.Tokheim@usn.no))

**Abstract:** The amount of CO<sub>2</sub> in the atmosphere is continuously increasing, resulting in climate change and global warming. Industrial processes contribute a substantial share in the amount of CO<sub>2</sub> released to the atmosphere. On the other hand, different types of wastes and by-products are being produced by different industries which are deemed pollutants and require energy and capital to be safely managed through a circular economy perspective. A solution to simultaneously tackle both the CO<sub>2</sub> emission and waste pollution problems would be of high value. CO<sub>2</sub> sequestration by mineralization of CaO-rich industrial wastes is one potential solution. In such a process, CO<sub>2</sub> reacts with the CaO in the waste and CaCO<sub>3</sub> is produced. This product is thermodynamically stable and has multiple uses. Many studies in the literature have reported use of various CaO-rich wastes to capture CO<sub>2</sub>, but they are mostly based on lab-scale experiments, and mostly the focus is on the chemistry of the suggested processes. Hence, there is a need to study the technical and economic feasibility of up-scaled industrial versions of such processes. In this study, four different aqueous indirect mineralization processes applying different chemicals, all with a relatively high performance documented from laboratory experiments, are scaled up to industrial size with a CO<sub>2</sub> capturing capacity of 400 t/y using an in-house-made process simulation tool. Furthermore, an economic analysis and environmental assessment are conducted for all processes, and the results are compared. Finally, parameters impacting the techno-economic feasibility of each process are evaluated through a sensitivity study. The results indicate that the potential of capturing CO<sub>2</sub> and producing CaCO<sub>3</sub> can be as high as 530 kg and 1200 kg per ton of the waste while the yearly energy consumption can be as low as 0.7 kWh per kilogram of captured CO<sub>2</sub>. The aqueous indirect mineralization of CO<sub>2</sub> can be profitable and the emitted CO<sub>2</sub> by the process can be so low as 6% of the captured amount.

**Keywords:** CO<sub>2</sub> sequestration, CO<sub>2</sub> capture, Mineralization, Aqueous indirect mineralization, Industrial wastes, Process simulation, Techno-economic analysis, Mass and energy balance, Environmental assessment

### 1. INTRODUCTION

Mineralization of silicates (Seifritz, 1990) is a direct process for carbonation and mineralization of natural alkaline minerals, such as olivine, serpentine and basalt, or industrial alkaline wastes like ashes and slags. This, due to the slow kinetics of mineral carbonation, needs a large energy demand to accelerate, or a long reaction time under ambient conditions. In addition, directly carbonating alkaline minerals usually produces low-quality products (Zhang et al., 2019).

On the other hand, there is the indirect carbonation process, which makes it possible to produce higher-value goods such as pure precipitated calcium carbonate (PCC) (Zhang et al., 2019). Indirect carbonation can be separated into aqueous indirect carbonation and stepwise gas-solid reactions. Prior to starting the mineral carbonation reaction, an indirect reaction must be used to extract alkaline earth metal ions from silicates

using the appropriate organic or inorganic acids or salts. Because the reactions usually occur in ambient conditions, this method may save energy in the mineral carbonation step. However, the extraction step (also known as the enrichment or separation step) may be uneconomical due to expensive reagents, reagent recovery, and energy consuming equipment (Zhang et al., 2019).

To determine which processes that have the lowest energy and cost intensity and the greatest amount of CO<sub>2</sub> captured, reaction modelling, process simulation, environmental impact assessment, energy analysis, and economic evaluation should be conducted. This will help determine the most promising options for scale-up (Zhang et al., 2020). Figure 1 shows a schematic overview of an indirect mineralization process.

Compared to solid phase mineralization methods, aqueous phase mineralization has demonstrated advantages in terms of

process operational parameters which are not under harsh conditions. Promising benefits of aqueous phase mineralization include the potential to speed up the process and the viability of large-scale implementation (Zhang et al., 2020).

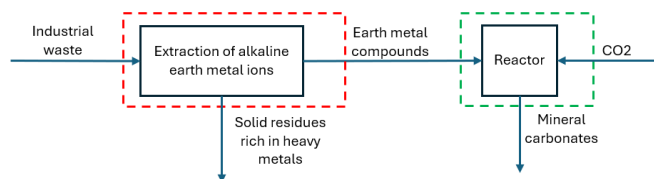


Fig. 1. A schematic overview of indirect mineralization process

The aqueous indirect mineralization of industrial wastes usually consists of two main steps. The first one is leaching, where the earth metal ions are separated from the waste. The second one is mineralization, where  $\text{CO}_2$  is introduced to the earth metal ions to be mineralized. Different wastes and methods based on literature have been used to perform the mentioned two steps. The waste can originate from various sources and the extracted earth metal could be different.

To extract the earth metal ions in the leaching process, an aqueous solution of acids or salts (reagents) with a specific concentration ( $C$ ) is prepared. Then, the solution is mixed with solids at a certain solid-to-liquid ratio ( $S:L$ ) at a specific leaching temperature ( $LT$ ) for a certain leaching time ( $TL$ ). The extraction efficiency ( $EF$ ) is defined as the part of the primary content of the earth metal ions which is extracted.

After the extraction, the  $\text{CO}_2$  is introduced to the solution, which is now rich in earth metal ions, at a specific mineralization temperature ( $MT$ ) for a certain mineralization time ( $TM$ ). In this way,  $\text{CO}_2$  is sequestered, and carbonates (mostly  $\text{CaCO}_3$ ) are produced. Appendix A gives details from the literature review done in this work.

In this study, the viability of aqueous indirect mineralization of  $\text{CO}_2$  by utilizing  $\text{CaO}$ -rich wastes for a plant in Norway with a  $\text{CO}_2$  capturing capacity of 400 t/y is investigated. The first step is, based on a literature study, to choose four processes with comparably good results. The second step is to model and simulate the chosen processes using an in-house-customized simulation tool (using MS Excel®) to solve mass and energy balances and do economic calculations. The third and final step is to define key performance indicators (KPI) and use these to compare the four processes in a sensitivity analysis. The work is based on a master's thesis work at USN (Ghazi, 2024).

## 2. PROCESS SELECTION

From the reviewed literature, the process using converter slag (CS) and  $\text{NH}_4\text{Cl}$  (Kodama et al., 2008) will be referred to as process 1, the process using recycled concrete fines (RCF) and  $\text{NH}_4\text{Cl}$  (Mehdizadeh et al., 2023) will be referred to as process 2, the process using blast furnace slag (BFS) and  $\text{HCl}$  (Liu et al., 2023) will be referred to as process 3, and the process using BFS and  $\text{CH}_3\text{COOH}$  (Teir et al., 2007) will be referred to as

process 4. These processes are chosen due to their comparably high  $\text{CaO}$  content in the wastes and high leaching efficiencies and because they use different reagents and apply different leaching and mineralization temperatures. For process 4, the  $MT$  and  $TM$  are not mentioned in the literature. Hence, the same values for  $LT$  and  $TL$  are assumed for these.

## 3. MODELLING AND SIMULATION

To be able to model and simulate the processes, first the processes are designed, and process flow diagrams (PFD) are prepared based on the details of the laboratory work in the papers. Then, using the PFDs, the mass and energy balance calculations can be conducted. Finally, based on mass and energy calculations, the economic and environmental assessment can be performed.

### 3.1 Process flow diagrams and descriptions

Figure 2 shows the PFD for process 1 and 4, and Table 1 provides the definitions of the streams in the PFD.

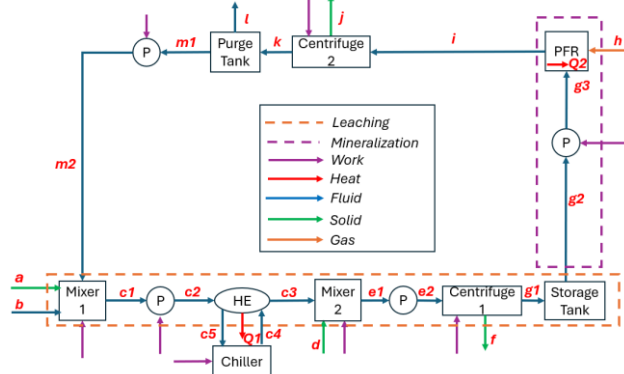


Fig. 2. Suggested PFD for process 1 and 4.

Table 1. Definition of streams in Fig. 2.

Stream	Definition
a	Reagent make-up
b	Water make-up
c1 and c2	Leaching solution
c4 and c5	Cooling water from chiller
c3	Cooled leaching solution
d	Industrial waste
e1 and e2	Leachate solution
f	Solid residues
g1, g2, and g3	Filtrate solution
h	$\text{CO}_2$
i	Mineralization solution
j	Precipitated $\text{CaCO}_3$
k	Recovered leaching solution
l	Purge
m1 and m2	Recovered leaching solution
Q1	Heat extracted from the process
Q2	Heat generated in the reactor

The water (b) and reagent (a and m2) are mixed in mixer 1, and the leaching solution (c1 and c2) is then pumped (P) through the heat exchanger (HE), where the stream is cooled down (Q1) to the leaching and mineralization temperature

using cooling water (c4 and c5) from a chiller. The leaching and mineralization temperatures are the same in process 1 and 4. After that, the industrial waste (d) is added to the leaching solution (c3) in mixer 2, where the leaching process happens in the leaching time. After leaching, the leachate (e1 and e2) is pumped (P) into centrifuge 1, where the solid residues (f) are separated, and the filtrate solution (rich in Ca) accumulates in the storage tank. Then the filtrate solution (g1, g2 and g3) is pumped (P) to the plug flow reactor (PFR), where CO<sub>2</sub> (h) is introduced to be mineralized, generating heat (Q2) due to exothermic nature of the reaction. After the PFR, the mineralization solution (i), containing CaCO<sub>3</sub>, passes through centrifuge 2, where the precipitated CaCO<sub>3</sub> (j) is separated from the stream. The recovered reagent (k) then accumulates in the purge tank, and a part of it (l) is purged out of the process to prevent accumulation of heavy metals and undesired materials. Finally, the recovered reagent (m1) is pumped (P) to mixer 1 to repeat the cycle.

Figure 3 depicts the suggested PFD for processes 2 and 3, and Table 2 provides the definition of streams that are different from those in Fig. 2. Processes 2 and 3 are quite similar to processes 1 and 4, but the operational temperatures are different. The leaching temperature is much higher than the mineralization temperature in processes 2 and 3. This requires the heat to be added to the stream before leaching to increase the temperature to the leaching temperature. Meanwhile, the heat must be removed from the stream before mineralization to reach the mineralization temperature. To reduce the heating and cooling demands, a heat recovery line using heat exchangers 1 (HE1) and 3 (HE3) is established to recover a part of the heat. The rest of the heat will be added to and will be removed from the stream using heat exchangers 2 (HE2) and 4 (HE4), respectively.

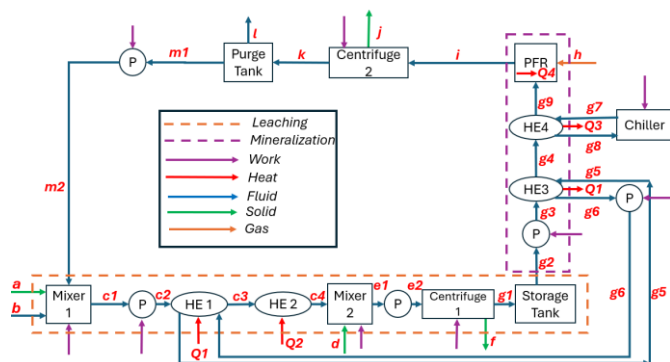


Fig. 3. Suggested PFD for process 2 and 3.

Table 2. Definition of streams in Fig. 3 that are new or different from those in Fig. 2.

Stream	Definition
c3 and c4	Cooled leaching solution
g5 and g6	Heat recovery line
g4 and g9	Cooled filtrate solution
g7 and g8	Cooling water from chiller
Q1	Recovered heat in the process
Q2	Heat added to the process
Q3	Heat extracted from the process
Q4	Heat generated in the reactor

### 3.2 Mass balance calculations

In the mineralization process, 1 mol of CO<sub>2</sub> reacts with 1 mol of CaO to produce 1 mol of CaCO<sub>3</sub>. Laboratory data from the literature, such as calcium content in the waste, reagent concentration, and solid-to-liquid ratio, are used to calculate flow rates, extraction efficiency and plant capacity for all the processes.

### 3.3 Energy balance calculations

The energy consumption of the four chosen processes is the sum of mechanical work (in pumps, agitators, mixers and centrifuges) and thermal energy related to heating and cooling demands. By knowing the mass flow rates, the power of agitators and centrifuges, the enthalpy of mineralization, and the specific heat capacity of the streams, the yearly energy consumption is calculated. Since the heat transfer area of the mixers, tanks, and pipes is not specified at this level, the heat loss from these equipment units is not calculated. Instead, the system is treated as well insulated, and heat loss is neglected.

### 3.4 Economic calculations

The economic calculations in this study are limited to material (reagent and process water) costs, energy cost, and revenue from sales of CaCO<sub>3</sub>. The mass flow rates of the required materials, the energy consumption, the energy price in Norway, and the reagent price (assuming three different origins; East Asia, the European Union, and the US) are used as inputs, see Appendix B for details. Then the revenue from sales of CaCO<sub>3</sub>, the yearly cost and the revenue of the processes are calculated. The economic assessment in terms of checking the profitability is then conducted.

### 3.5 CO<sub>2</sub> footprint

Although the CO<sub>2</sub> footprint of a process depends on numerous factors and aspects, in this study, the CO<sub>2</sub> footprint calculated based on the electrical energy consumption, assumed to be only electricity from grid. The CO<sub>2</sub> emission factors of electricity in the country where the plants are located are given in Appendix B.

### 3.6 Simulation tool and simulation settings

Laboratory data from the literature are used as inputs to the mass and energy balance equations. Assumptions are made where sufficient data are not available. Then a simulation tool is implemented in MS Excel<sup>®</sup> to calculate and scale up the unknowns, such as mass flow rates, energy consumption, etc. This tool is also used to perform the sensitivity analysis. The simulation settings are shown in appendix B.

## 4. KEY PERFORMANCE INDICATORS

To illustrate and compare the performance of the processes, eight KPIs are defined in Table 3 based on the results of mass, energy, economic, and environmental calculations.

KPIs 1 to 3 are mass-based and can be used to compare how much CO<sub>2</sub> that can be captured, how much waste that can be handled and how much make-up reagents that are required. KPI1 and KPI2 should be high, whereas KPI3 should be low.

Table 3. KPIs and their definitions.

KPI	Definition
KPI1	Mass of captured CO <sub>2</sub> per mass of waste
KPI2	Mass of produced CaCO <sub>3</sub> per mass of waste
KPI3	Mass of make-up reagent per mass of captured CO <sub>2</sub>
KPI4	Energy consumption per mass of captured CO <sub>2</sub>
KPI5	Mass of produced CO <sub>2</sub> per mass of captured CO <sub>2</sub>
KPI6	Yearly profit per mass of captured CO <sub>2</sub> if the reagent is supplied from East Asia
KPI7	Yearly profit per mass of captured CO <sub>2</sub> if the reagent is supplied from the EU
KPI8	Yearly profit per mass of captured CO <sub>2</sub> if the reagent is supplied from the US

KPI4 is energy-based and can be used to compare how much energy that must be supplied to the different processes. This value should be low.

KPI5 is also mass-based, but the main aim of this parameter is to show the environmental impact of the processes; the lower the better. KPIs 6 to 8 are used to compare the economic performance of the processes, the higher values the better.

## 5. RESULTS AND DISCUSSION

### 5.1 Mass balance results

The calculated mass flow results for the streams in the four processes are shown in Table 4.

Although the CO<sub>2</sub> and CaCO<sub>3</sub> streams (h and j) are the same in all four processes, other streams are different. Taking g1 as for comparison, process 4 has the highest flow rate of 159 kg/min, which is the double of the flow rate in process 1 with 81 kg/min. The lowest flow rate is for process 2 with 24 kg/min. This will result in a higher energy consumption of the pumps and centrifuges. Considering stream a, process 4 has the highest consumption of reagent followed by processes 3, 1, and 2. The higher the reagent consumption, the higher the process costs.

### 5.2 Energy balance

The energy consumption results for the four processes are shown in Table 5. Compared to other rotary equipment, the pump energy consumption is negligible in all four processes. For process 4, the energy consumption of the centrifuges is almost twice as high as in process 1. This is due to a higher flow rate in process 4. Heating and cooling, with more than 70 % of the whole energy consumption, are the main role-players in the energy consumption of processes 2 and 3.

Table 4. Mass flow rates (kg/min) (– = Not applicable)

Stream	Process			
	1	2	3	4
a	0.6	0.4	0.8	2.4
b	8	2.3	3.7	16
c1 and c2	80	23	37	158
c3	80	23	37	158
c4	22	23	37	67
c5	22	–	–	67
d	5.0	2.3	3.0	2.7
e1 and e2	85	25	40	161
f	4.3	1.5	2.2	1.9
g1, g2, and g3	81	24	38	159
g5 and g6	–	25	39	–
g4 and g9	–	24	38	–
g7 and g8	–	123	151	–
h	0.8	0.8	0.8	0.8
i	82	25	39	160
j	1.7	1.7	1.7	1.7
k	80	23	37	158
l	8	2.3	3.7	16
m1 and m2	72	21	33	142

Table 5. Energy streams (kW) (– = Not applicable)

Utility	Process			
	1	2	3	4
Agitation	15	15	15	15
Pumps	0.06	0.02	0.03	0.12
Centrifuges	14	4	6	26
Heating	–	31	49	–
Cooling (Chiller)	10	17	20	10
Total energy	39	67	91	51

### 5.3 KPI results

The mass and energy balance results are used, along with cost and environmental calculations, in the calculation of KPIs. Figure 4 shows KPIs 1 to 3 and 5.

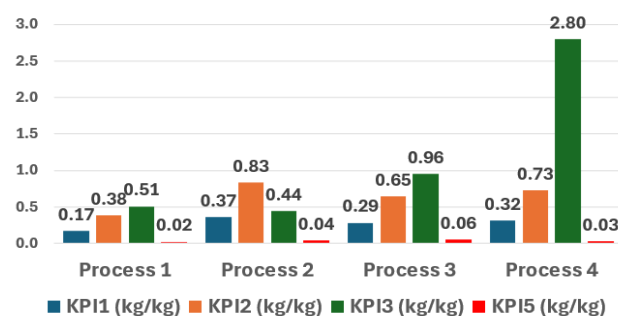


Fig. 4. KPIs 1, 2, 3, and 5



As shown in Fig. 4, process 2 has the highest capacity of capturing CO<sub>2</sub> per mass of used waste (KPI1) with 0.37 kg/kg. Process 4 and 3 follow with values of 0.32 kg/kg and 0.29 kg/kg, respectively. Process 1 has the lowest potential of capturing CO<sub>2</sub> with only 0.17 kg/kg.

The trend for KPI2 is similar to that of KPI1; process 2 has the highest amount of produced CaCO<sub>3</sub> per mass of waste (0.83 kg/kg) followed by processes 4, 3, and 1 (0.73, 0.65, and 0.38 kg/kg, respectively).

The reasons for the higher capacity for CO<sub>2</sub> capture and CaCO<sub>3</sub> production of process 2 is the higher content of CaO in the waste, a higher solid-to-liquid ratio, and a higher extraction efficiency. Although the waste CaO content of process 1 is almost the same as in processes 3 and 4, the lower extraction efficiency results in a lower capture capacity.

When it comes to KPI3, the lower mass of make-up reagent per mass of captured CO<sub>2</sub>, the better in terms of economic assessment. Hence, process 2 is still the better process, with a reagent consumption of 0.44 kg/kg, followed by process 1 with 0.51 kg/kg and process 3 with 0.96 kg/kg. Process 4 has a staggeringly high reagent consumption of 2.8 kg/kg. Although the concentration of reagent for this process is not high compared to the other three processes, the comparably lower solid-to-liquid ratio results in a higher volume of leaching solution which increases the reagent consumption.

KPI5 is an indicator of the emitted mass of CO<sub>2</sub> per mass of captured CO<sub>2</sub>. This KPI is of high importance and should be calculated in the early stages of a scale-up project since it can be a showstopper. If KPI5 shows 1 kg/kg or more, it means that the plant is emitting more CO<sub>2</sub> than it captures. This depends on the CO<sub>2</sub> emission factor of electricity generation. Figure 4 shows KPI5 for power production in Norway, which has a very low CO<sub>2</sub> emission factor. Accordingly, all four processes emit negligibly low amounts of CO<sub>2</sub> per unit of captured CO<sub>2</sub> with 0.02 kg/kg, 0.03 kg/kg, 0.04 kg/kg, and 0.06 kg/kg for processes 1, 4, 2, and 3, respectively.

Based on Fig. 5, processes 1 and 4 are the most efficient ones in terms of energy consumption per mass of captured CO<sub>2</sub> with 0.86 kWh/kg and 1.13 kWh/kg followed by process 2 (1.47 kWh/kg) and process 3 (1.98 kWh/kg).

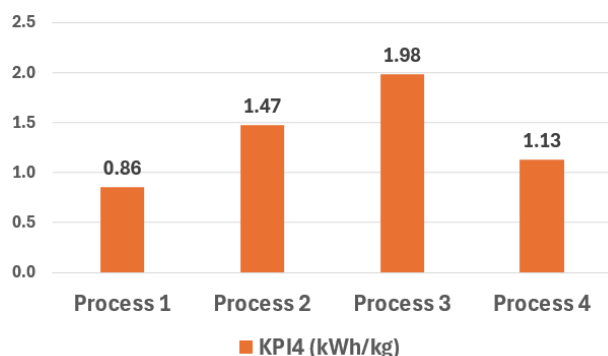


Fig. 5. KPI4 for all processes

Interestingly, despite higher mass flow rates for processes 1 and 4, which result in a higher energy consumption of pumps and centrifuges, the total energy consumption of these two processes is lower than processes 2 and 3. This is due to different operational temperatures of leaching and mineralization in processes 2 and 3, which require heating and cooling at the same time, resulting in a higher overall energy consumption for these two processes.

The mass of captured CO<sub>2</sub> and produced CaCO<sub>3</sub> are the same for all four processes. Therefore, the revenue from sales of CaCO<sub>3</sub> is also the same for all. Figure 6 shows the yearly profit of all four processes per mass of captured CO<sub>2</sub> if the reagents are supplied from East Asia (KPI6), the EU (KPI7), and the US (KPI8).

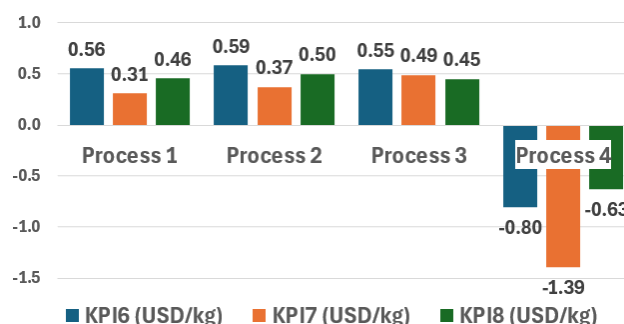


Fig. 6. KPIs 6 to 8, economic assessment

Process 4 shows negative numbers for all three KPIs, meaning that the costs are higher than the revenue, and the process is not profitable. For KPIs 6 to 8, process 1, 2, and 3 are all profitable. The profitability is highest if the reagent is supplied from East Asia (0.59 USD/kg for process 2), and lowest if it is supplied from the EU (0.31 USD/kg for process 1). This can be explained by different chemical prices (see Appendix B).

#### 5.4 Sensitivity analysis

The reactants in the mineralization reaction are CO<sub>2</sub> and CaO. Since the amount of CO<sub>2</sub> to be captured is a design basis value (400 kt/y) in this study, the amount of CaO plays the main role in the mass and energy balance calculations. The amount of CaO, or better Ca<sup>2+</sup> ions in the reaction, is dependent on the extraction efficiency at a given solid-to-liquid ratio. Due to the importance of the extraction efficiency, a sensitivity analysis was conducted to find the impact of this parameter on KPIs 1-4. The extraction efficiency was varied from 8 to 98 %, and the results are shown in Figs. 7 to 10. (The reported efficiencies from the laboratory work are indicated with \* on the horizontal axis in the figures.)

As seen from all four figures, KPIs 1 and 2 have a linearly increasing trend with an increase in the extraction efficiency. This means that the extraction efficiency has a direct impact on the capturing capacity of each process. This trend is reasonable since the extracted Ca is directly reacting with CO<sub>2</sub>. KPIs 3 and 4, on the other hand, show an exponential decay behavior with an increase in the extraction efficiency. The non-linear behavior is seen because there is more than one role-player in the calculation of make-up reagent and the

energy consumption, and these two KPIs are sum of different parameters. The decreasing trend occurs because the reagent and energy consumption are reduced when the extraction efficiency is increased.

Looking into KPIs 1 and 2 for the whole range of extraction efficiencies, process 2 is the more promising one. Doing the same for KPIs 3 and 4, process 1 is the preferred process.

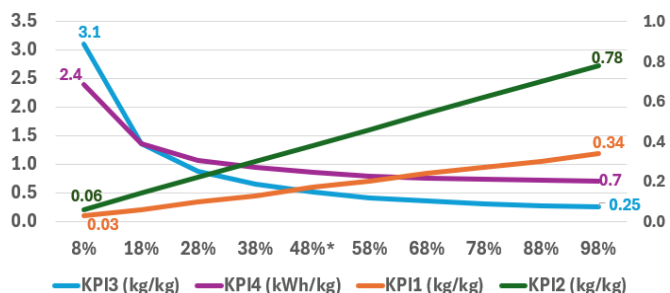


Fig. 7. Sensitivity analysis of process 1

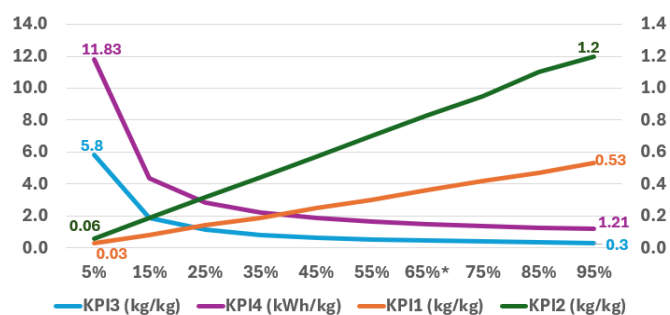


Fig. 8. Sensitivity analysis of process 2

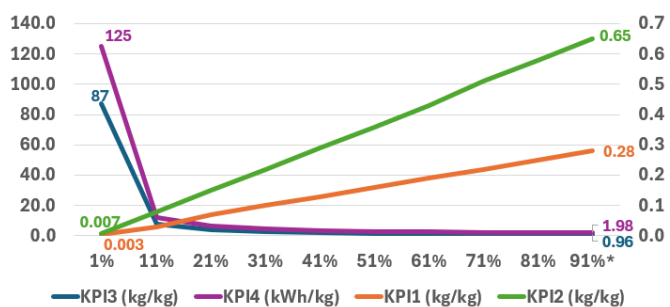


Fig. 9. Sensitivity analysis of process 3

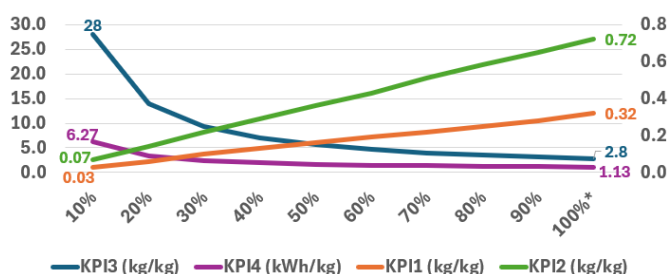


Fig. 10. Sensitivity analysis of process 4

In Fig. 11, the processes are compared at an extraction efficiency of 50 %. While process 2 has a better performance for KPIs 1 and 2, process 1 is better for KPIs 3 and 4.

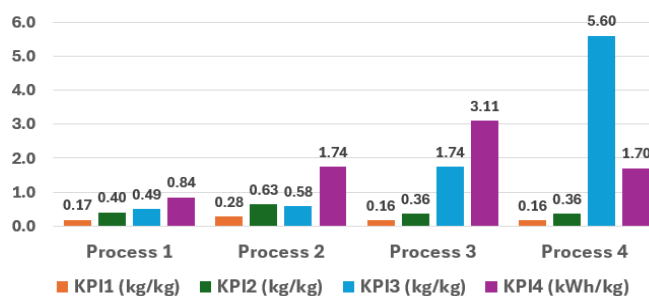


Fig. 11. KPIs 1 to 4 at EF=50% for all processes

## 6. CONCLUSIONS

Many methods to mineralize CO<sub>2</sub> by industrial CaO-rich waste streams have been described in the literature, mainly based on laboratory experiments. In this study, four different processes were selected, scaled up to industrial scale and compared.

The results indicate that a process using recycled concrete fines (RCF) and NH<sub>4</sub>Cl as a solvent (process 2) has the highest specific CO<sub>2</sub> capture (KPI1) and CaCO<sub>3</sub> production (KPI2) and the lowest chemical make-up requirement (KPI3).

However, a process using converter slag (CS) and NH<sub>4</sub>Cl as solvent (process 1) has the lowest specific energy consumption (KPI4).

The two other processes considered were using blast furnace slag (BFS) and either HCl (process 3) or CH<sub>3</sub>COOH as a solvent (process 4). All four processes will generate less than 6 % of the CO<sub>2</sub> that is captured (KPI5), meaning that they are all viable from net CO<sub>2</sub> capture point of view.

The analysis indicated that process 4 is not economically viable, not matter if the chemicals are supplied from East Asia (KPI6), the EU (KPI7) or the US (KPI8). Processes 1-3 all appear to be economically viable, irrespective of where the chemical reagent is purchased.

This study indicates that CO<sub>2</sub> mineralization using industrial by-products may be part of a solution going towards a more circular economy. However, as only operational costs were included in the present analysis, the impact of including investment costs could be investigated in a future study.

## ACKNOWLEDGEMENTS

We kindly thank Mr. Zahir Barahmand from University of South-Eastern Norway for his advice on the literature study, Dr. Eugenia Marinou, and Mr. Ole Jakob Sandal from Caux AS for valuable discussions on mineralization and making the opportunity for this study available.

## REFERENCES

- businessanalytiq, Ammonium chloride price index. URL <https://businessanalytiq.com/procurementanalytics/index/ammonium-chloride-price-index/> (accessed 4.24.24).
- Carbon intensity of electricity generation [WWW Document], Our World in Data. URL <https://ourworldindata.org/grapher/carbon-intensity-electricity> (accessed 4.25.24).

- Electricity prices [WWW Document], SSB. URL <https://www.ssb.no/en/energi-og-industri/energi/statistikk/elektrisitetspriser> (accessed 4.24.24).
- Gao, Y., Jin, X., Teng, L., Rohani, S., He, M., Li, J., Ren, S., Liu, Q., Huang, J., Duan, H., Xin, Y., and Liu, W. (2023). CO<sub>2</sub> mineral sequestration and nickel recovery from laterite ore by using waste copperas. *Fuel*, 331, 125750. doi: 10.1016/j.fuel.2022.125750
- Ghazi, A., (2024). CO<sub>2</sub> capture through mineralization of CaO-containing by-products. University of South-Eastern Norway, Porsgrunn, Norway.
- Ho, H.-J., Iizuka, A., Shibata, E., and Ojumu, T. (2022). Circular indirect carbonation of coal fly ash for carbon dioxide capture and utilization. *Journal of Environmental Chemical Engineering*, 10, 108269. doi: 10.1016/j.jece.2022.108269
- Ji, L., Zheng, X., Ren, Y., Wang, Yikun, Wang, Yan, and Yan, S., (2024). CO<sub>2</sub> sequestration and recovery of high-purity CaCO<sub>3</sub> from bottom ash of masson pine combustion using a multifunctional reagent—amino acid. *Separation and Purification Technology* 329, 125171. doi: 10.1016/j.seppur.2023.125171
- Kashefi, K., Pardakhti, A., Shafiepour, M., and Hemmati, A., (2020). Process optimization for integrated mineralization of carbon dioxide and metal recovery of red mud. *Journal of Environmental Chemical Engineering*, 8, 103638. doi:10.1016/j.jece.2019.103638
- Kim, M.-J., Jeon, J., (2020). Effects of Ca-ligand stability constant and chelating agent concentration on the CO<sub>2</sub> storage using paper sludge ash and chelating agent. *Journal of CO<sub>2</sub> Utilization*, b 40, 101202. doi: 10.1016/j.jcou.2020.101202
- Kodama, S., Nishimoto, T., Yamamoto, N., Yogo, K., and Yamada, K., (2008). Development of a new pH-swing CO<sub>2</sub> mineralization process with a recyclable reaction solution. *Energy*, 33, 776–784. doi: 10.1016/j.energy.2008.01.005
- Lin, Y., Yan, B., Mitas, B., Li, C., Fabritius, T., and Shu, Q., (2024). Calcium carbonate synthesis from Kambara reactor desulphurization slag via indirect carbonation for CO<sub>2</sub> capture and utilization. *Journal of Environmental Management*, 351, 119773. doi: 10.1016/j.jenvman.2023.119773
- Liu, L., Gan, M., Fan, X., Sun, Z., Wei, J., Li, J., and Ji, Z., (2023). Synthesis of high-value CaCO<sub>3</sub> via indirect CO<sub>2</sub> fixation utilized blast furnace slag. *Journal of Environmental Chemical Engineering*, 11, 110655. doi: 10.1016/j.jece.2023.110655
- Mehdizadeh, H., Mo, K.H., and Ling, T.-C., (2023). O<sub>2</sub>-fixing and recovery of high-purity vaterite CaCO<sub>3</sub> from recycled concrete fines. *Resources, Conservation and Recycling*, 188, 106695. doi: 10.1016/j.resconrec.2022.106695
- Recycling, 188, 106695. doi: 10.1016/j.resconrec.2022.106695
- Proaño, L., Sarmiento, A.T., Figueredo, M., and Cobo, M. (2020). Techno-economic evaluation of indirect carbonation for CO<sub>2</sub> emissions capture in cement industry: A system dynamics approach. *Journal of Cleaner Production*, 263, 121457. doi: 10.1016/j.jclepro.2020.121457
- Seifritz, W. (1990). CO<sub>2</sub> disposal by means of silicates. *Nature*, 345, 486–486. doi: 10.1038/345486b0
- Song, Q., Guo, M.-Z., and Ling, T.-C. (2024). Synthesis of High-Purity and Stable Vaterite Via Leaching-Carbonation of Basic Oxygen Furnace Slag. *ACS Sustainable Chemistry and Engineering*, 12, 4081–4091. doi: 10.1021/acssuschemeng.3c07375
- Szepessy, S. and Thorwid, P. (2018). Low Energy Consumption of High Speed Centrifuges. *Chemical Engineering & Technology*, 41. doi: 10.1002/ceat.201800292
- Teir, S., Eloneva, S., Fogelholm, C.-J., and Zevenhoven, R. (2007). Dissolution of steelmaking slags in acetic acid for precipitated calcium carbonate production. *Energy, ECOS 05. 18th International Conference on Efficiency, Cost, Optimization, Simulation, and Environmental Impact of Energy Systems* 32, 528–539. doi: 10.1016/j.energy.2006.06.023
- Wang, N., Feng, Y., and Guo, X. (2020). Atomistic mechanisms study of the carbonation reaction of CaO for high-temperature CO<sub>2</sub> capture. *Applied Surface Science*, 532, 147425. doi:10.1016/j.apsusc.2020.147425
- Wu, L., Li, H., Mei, H., Rao, L., Xia, Y., and Dong, Y. (2023). A novel approach to accelerate carbon dioxide sequestration of ladle furnace slag using sodium bicarbonate solution. *Minerals Engineering* 204, 108374. doi: 10.1016/j.mineng.2023.108374
- Yiyimechanical.com [WWW Document], Yiyi Machinery. URL <https://www.yiyimechanical.com/shop/mixing-tank> (accessed 5.18.24).
- Zhang, N., Chai, Y.E., Santos, R.M., and Šiller, L. (2020). Advances in process development of aqueous CO<sub>2</sub> mineralisation towards scalability. *Journal of Environmental Chemical Engineering*, 8, 104453. doi: 10.1016/j.jece.2020.104453
- Zhang, N., Santos, R.M., Smith, S.M., and Šiller, L. (2019). Acceleration of CO<sub>2</sub> mineralisation of alkaline brines with nickel nanoparticles catalysts in continuous tubular reactor. *Chemical Engineering Journal, ISCRE 25 Special Issue: Bridging Science and Technology*, 377, 120479. doi: 10.1016/j.cej.2018.11.177

## Appendix A: Literature review details

Waste Type	Metal	Content (%)	Reagent	C (mol/L)	S:L (g/L)	LT (°C)	TL (min)	EF (%)	MT (°C)	TM (min)	Reference
Biomass ash	Ca	CaO: 36.7	Glycine	2	300	25	60	19.9	25	60	Ji et al., 2024
Kambara reactor desulphurization slag	Ca	CaO: 72.04	NH <sub>4</sub> Cl	0.5	10	25	120	89.76	40	120	Lin et al., 2024
Recycled concrete fines (RCF)	Ca	CaO: 71.11	NH <sub>4</sub> Cl	2	100	85	60	65.7	25	30	Mehdizadeh et al., 2023
Converter slag (CS)	Ca	CaO: 44.5	NH <sub>4</sub> Cl	1	63	80	60	48.1	80	120	Kodama et al., 2008
Blast furnace slag (BFS)	Ca	CaO: 40	HCl	4	80	80	120	91	20	15	Liu et al., 2023
Blast furnace slag (BFS)	Ca	CaO: 40.6	CH <sub>3</sub> COOH	1.7	16.8	25	120	100	N/A	N/A	Teir et al., 2007
Laterite Ore Copperas	Mg	MgO: 37.11	Distilled water	N/A	100	80	60	86	30	120	Gao et al., 2023
Coal fly ash	Ca	Ca: 3.44	HNO <sub>3</sub>	0.3	30	25	150	72.6	25	30	Ho et al., 2022
Ladle furnace slag	Ca	CaO: 46.73	NaHSO <sub>4</sub>	0.5	143	25	90	N/A	25	120	Wu et al., 2023
Basic oxygen furnace slag (BOF)	Ca	CaO: 40	NH <sub>4</sub> Cl	2	50	80	10	60.3	25	10	Song et al., 2024
Red mud	Ca	CaO: 14.21	HCl	1	70	80	120	85	25	N/A	Kashefi et al., 2020
Paper sludge ash (PSA)	Ca	Ca: 67.2	Citrate	0.1	20	25	60	23.5	25	N/A	Kim and Jeon, 2020



## Appendix B: Simulation inputs

Input	Process 1	Process 2	Process 3	Process 4	Reference
Captured CO <sub>2</sub> (t/y)	400	400	400	400	Assumed
CaO content of waste (%)	44.5	71.11	40	40.6	Kodama et al., 2008, Mehdizadeh et al., 2023 Liu et al., 2023, Teir et al., 2007
S/L (g/L)	63	100	80	16.8	Kodama et al., 2008, Mehdizadeh et al., 2023 Liu et al., 2023, Teir et al., 2007
EF (%)	48.1	65.7	91	100	Kodama et al., 2008, Mehdizadeh et al., 2023 Liu et al., 2023, Teir et al., 2007
Purge fraction (%)	10	10	10	10	Assumed
LT (°C)	80	85	80	25	Kodama et al., 2008, Mehdizadeh et al., 2023 (Liu et al., 2023) (Teir et al., 2007)
MT (°C)	80	25	20	25	Kodama et al., 2008, Mehdizadeh et al., 2023 Liu et al., 2023, Teir et al., 2007
Specific heat capacity of streams (kJ/kgK)	4.2	4.2	4.2	4.2	Assumed
Enthalpy of mineralization (kJ/mol)	178	178	178	178	Wang et al., 2020
Centrifuge energy consumption (kWh/m <sup>3</sup> )	1.5	1.5	1.5	1.5	Szepessy and Thorwid, 2018
Density of streams (kg/m <sup>3</sup> )	1000	1000	1000	1000	Assumed
Agitator power (kW)	7.5	7.5	7.5	7.5	“yiyimechanical.com,” n.d.
Head loss (m)	5	5	5	5	Assumed
CO <sub>2</sub> production in Norway (kg/kWh)	0.029	0.029	0.029	0.029	“Carbon intensity of electricity generation,” n.d.
Energy price in Norway (USD/MWh)	42.63	42.63	42.63	42.63	“Electricity prices,” n.d.
Reagent price in East Asia (USD/kg)	0.08	0.08	0.04	0.47	businessanalytiq, n.d.
Reagent price in the EU (USD/kg)	0.56	0.56	0.1	0.68	businessanalytiq, n.d.
Reagent price in the US (USD/kg)	0.27	0.27	0.14	0.41	businessanalytiq, n.d.
Process water cost (USD/kg)	0.00755	0.00755	0.00755	0.00755	Proaño et al., 2020
Price of CaCO <sub>3</sub> (USD/kg)	0.31	0.31	0.31	0.31	Proaño et al., 2020